Egypt. J. Phys. **Vol. 51,** pp. 135-149 (2023)

Egyptian Journal of Physics

https://ejphysics.journals.ekb.eg/

AC conductivity Mechanism and Dielectric Relaxation of Bulk Titanium Phthalocyanine Chloride ($TiPcCl_2$)

Sabrien M. Abdelhamid*, M. Dongol, A. F. Elhady, Amr Attia Abuelwafa

Nano and Thin film lab. Physics Department, Faculty of Science, South Valley University, Qena 83523, Egypt

Abstract

The X-ray diffraction patterns (XRD) indicate that the powder of Titanium phthalocyanine chloride exhibits a polycrystalline nature, characterized by a triclinic structure. The AC electrical conductivity and dielectric properties of a bulk TiPcCl2 sample in pellet form were examined using evaporated ohmic Ag electrodes in a temperature range (293- 363K) and frequency range (50 HZ- 5 MHz). The frequency dependence of σ_{AC} follows the Jonscher's universal dynamic law with the relation $\sigma_{AC} = A\omega^s$, where s is the frequency exponent. The observed value of s is less than a unit and decreases as the temperature rises, which was consistent with the correlated barrier hopping (CBH) model. The barrier height W_M was determined. It is found also that $\ln\sigma_{AC}$ increases linearly with the reciprocal of the absolute temperature. This indicated that the AC conductivity is thermally activated process. The dielectric constant, ε_1, and the dielectric loss, ε_2, for bulk $TiPcCl_2$ both dropped as frequency increases and rose as temperature rises. The dielectric modulus serves as an indicator for the existence of non-Debye relaxation events within the material. The relaxation periods, ascertained through analysis of the imaginary component of the modulus (M``), were found to conform to the Arrhenius equation.

Keywords: Organic semiconductor; $TiPcCl_2$; Dielectric properties; AC conductivity.

***Corresponding author**
E-mail: sabrienmahmoud@sci.svu.edu.eg

Introduction

Organic electrical technologies are widely employed in our everyday lives. Phthalocyanines (Pcs) and Metalphthalocyanines (MPcs) are a promising and well-known organic dye with several potential advantages such as easy processing, high flexibility, high stability, etc. [1–4]. In general, MPcs play an important role in a wide range of scientific and technical applications. PCs may be used instead of conventional semiconductors to make low-cost devices such as optical filters, organic light emitting diodes, solar cell and gas sensors. [2–6].

The conduction mechanism, charge carrier transport mechanism, and polarisation types present in organic materials can be effectively characterised using dielectric and alternating current (AC) conductivity tests [7,8]. The

*Corresponding author: Sabrien M. Abdelhamid, E-mail: sabrienmahmoud339@gmail.com, Tel.: +2 01014220405
Received: 27/08/2023; Accepted: 03/09/2023
DOI: 10.21608/EJPHYSICS.2023.230926.1092

examination of dielectric characteristics plays a vital role in ascertaining the inherent qualities of barriers. Furthermore, a comprehensive understanding of the dielectric constant, dielectric relaxation, and conductivity of the materials involved might potentially enhance the investigation of the product's structure, quality, flaws, processing, and control. The frequency-dependent AC conductivity, denoted as $\boldsymbol{\sigma_{AC}(\omega)}$, in most semiconductors exhibits a power-law relationship with frequency, as described by Jonscher's power-law equation $\boldsymbol{\omega^s}$, where s is the frequency exponent. To elucidate the mechanisms underlying conductivity, the analysis of the temperature and frequency-dependent relationship of the frequency exponent, denoted as s, relies on the assessment of the relaxation induced by the tunnelling or hopping of charge carriers between equilibrium sites. This investigation aims to provide a comprehensive understanding of the conductivity mechanisms. According to sources [9]–[11].

The frequency exponent, denoted as s, in the quantum mechanical tunnelling (QMT) model, is contingent upon the frequency and remains unaffected by changes in temperature. The appropriateness of the overlapping big polaron tunnelling model arises when the frequency exponent, denoted as s, has a dependence on both frequency and temperature. Specifically, the exponent s decreases as temperature increases up to a specific threshold, beyond which it starts to increase with further temperature increments. Moreover, it should be noted that the frequency exponent, denoted as s, exhibits an increase when the temperature escalates in the context of tiny polaron tunnelling. In the context of the correlated barrier hopping (CBH) model, the frequency exponent, denoted as s, has a value less than unity, and it decreases with increasing temperature. Nevertheless, the conventional hopping model assumes a constant value of unity for the frequency exponent, denoted as **s.** Many researchers have focused on the AC conductivity and dielectric characteristics of Metalphthalocyanines (MPcs) compounds in order to explore the electrical conduction process as a function of frequency and temperature such as PdPc [12], MgPc [13], Na_2Pc [14] ZnPc [15], CuPc [16], CoPc [17], FePc [18], and AlPcCl [19]. According to our best knowledge, neither the electrical nor the dielectric characteristics of $TiPcCl_2$ have ever been investigated. As a result, the focus of this work has been on the investigation of the AC conductivity of $TiPcCl_2$ pellets at temperatures ranging from 293 to 363 K and throughout a frequency range of 50 Hz to 5 MHz. The electric modulus, dielectric constant, and dielectric loss have been determined using a variety of theoretical models.

Experimental techniques

The $TiPcCl_2$ (see **Scheme 1**) powder was acquired from the Sigma-Aldrich Company. The substance was thoroughly pulverised using a mortar, resulting in the formation of highly minute particles. These particles were subsequently subjected to a compression force of 1.96×10^8 N/m^2, resulting in the formation of a pellet with a diameter of 3mm and a thickness of 1mm. In order to establish an ohmic contact with the sample, a pellet of $TiPcCl_2$ was inserted between two electrodes consisting of evaporated Ag film (see Scheme 1). The AC dielectric data in the frequency range of 50 Hz to 5 MHz was measured using the (**Hioki 3536 Hitester**) an automatic RLC Bridge model. The specimen was positioned within a specialized holder featuring a distinct design, aimed at minimizing the occurrence of stray capacitance. The temperature of the $TiPcCl_2$ sample was measured throughout a range extending from ambient temperature to 363 K.

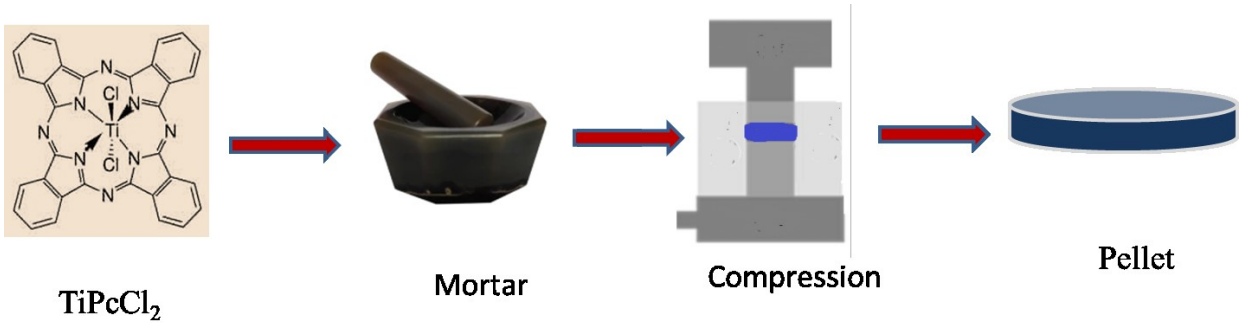

Scheme 1: Experimental setup for single-pellet compression from $TiPcCl_2$

Results and Discussions

Structural studies

The poly crystalline nature of the obtained powder of $TiPcCl_2$ is determined through structural analyses utilizing the X-ray diffraction (XRD) technique, as depicted in **Fig. 1**. The X-ray diffraction (XRD) pattern of the powdered sample exhibited many diffraction peaks. The determination of Miller indices for all observed peaks and the calculation of lattice constants for $TiPcCl_2$ are achieved using the CRYSFIRE and CHECKCELL software programs. The diffraction pattern analysis reveals that $TiPcCl_2$ possesses a triclinic structure with the space group p_1^- and lattice constants of a = 11.02 Å, b = 12.52 Å, c = 10.45 Å, α = 96.05°, β = 117.38°, and γ = 108.45°.

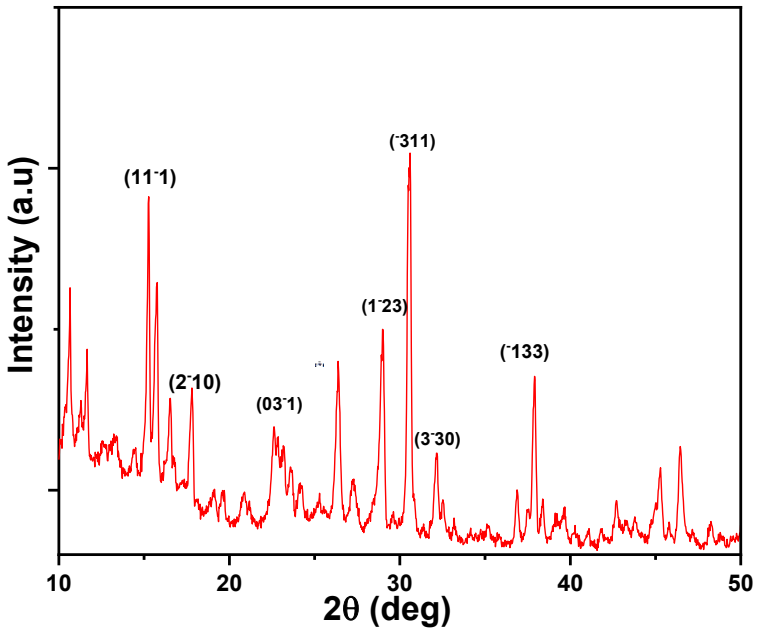

Fig. 1. X-ray diffraction patterns of $TiPcCl_2$in powder form.

AC conductivity studies

The use of AC conductivity measurements is widely recognised as an essential tool in the investigation and acquisition of precise insights into the underlying process of charge transport in semiconductor materials. The total conductivity, σ_t (ω,T), of semiconducting materials is described by the transition between the dispersive high-frequency regions to the low-frequency DC plateau [20]. The total conductivity $\sigma_t(\omega,T)$ was determined using the following formula: $\sigma_t(\omega,T) = d/ZA$, where d is the sample's thickness and A is its cross-sectional area. **Fig.2** represents the reliance of $ln\sigma_{tot}$ of $TiPcCl_2$ on a wide range of frequencies at various temperatures. The figure shown in this analysis reveals a positive correlation between conductivity and both temperature and frequency. Furthermore, the conductivity curves are divided into two distinct zones, namely the I and II regions. In area I, there is a positive correlation between temperatures, frequency, and conductivity, with the latter exhibiting a little increase as temperatures and frequency increase. The conductivity in area II experiences a quick increase as the frequency increases, owing to the much shorter duration of the electric field in this region. This behaviour is consistent with other semiconductors [12],[21],[22].

The AC conductivity $\sigma_{ac}(\omega,T)$ was computed with the use of the relation:

$$\sigma_{tot}(\omega, T) = \sigma_{DC}(T) + \sigma_{AC}(\omega, T) \quad (1)$$

Where σ_{dc} is the direct current (dc) conductivity, which is independent of frequency. Its values can be obtained by extrapolating the experimental data of σ_t at low frequency down to zero value as shown in **Fig 3** while σ_{ac} in equ (1) is the alternating current (ac) conductivity, which varies with frequency. The values of $\sigma_{ac}(\omega)$ at different temperatures can be determined as are shown in **Fig 4**.

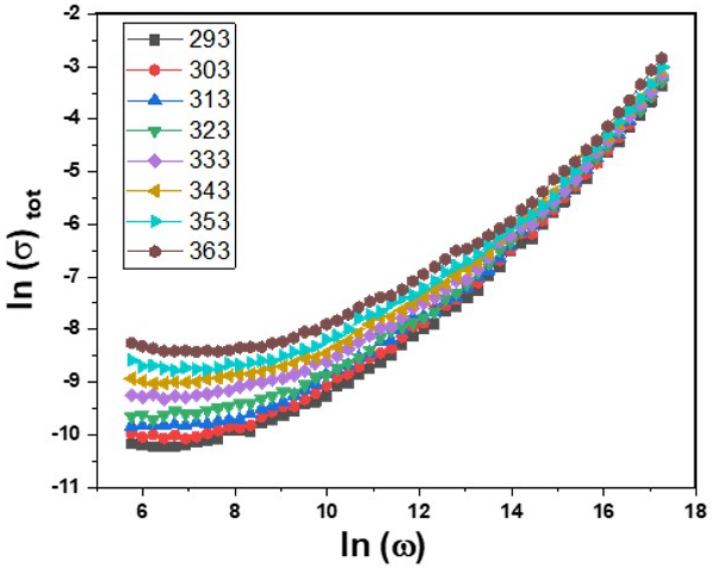

Fig .2. Frequency dependence of σ_{total} for $TiPcCl_2$ at different temperatures.

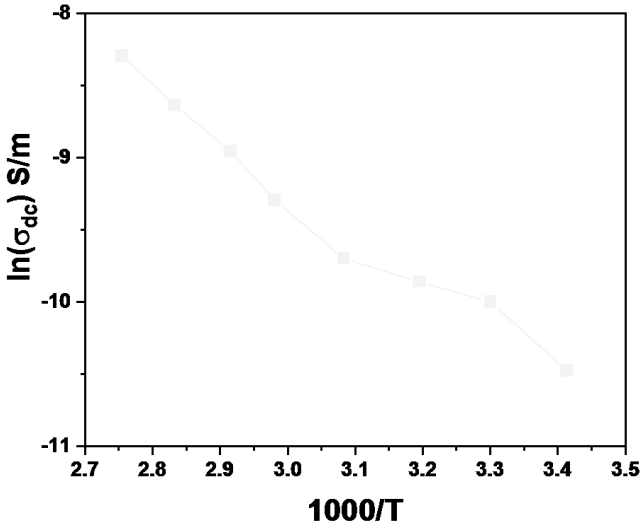

Fig. 3. Temperature dependence of DC conductivity of $TiPcCl_2$.

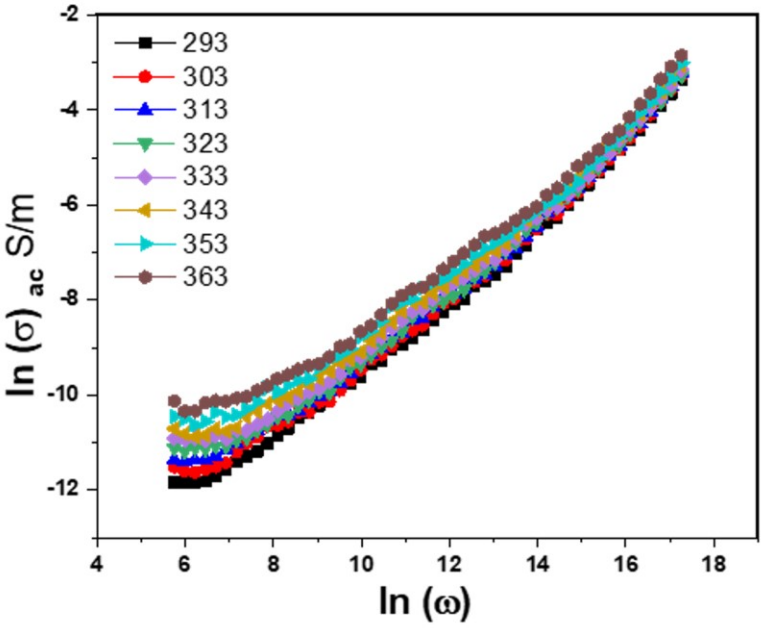

Fig. 4. Frequency dependence of σ_{AC} for $TiPcCl_2$ at different temperatures.

This can be described using the following equation:

$$\sigma_{ac}(\omega) = A\omega^{s} \qquad (2)$$

where ω is the angular frequency, *A* is the temperature constant, and *s* is the frequency exponent. According to Eq (2) σ_{ac} grows with increasing frequency and temperature as shown in **Fig .4** The slope of the linear $ln(\sigma_{ac})$ vs. $ln(\omega)$ plot is used to calculate the values of s which was drown at various temperatures as shown in **Fig .5**.

The provided figure presents two noteworthy observations: firstly, a negative correlation between the variable s and temperature, indicating a reduction in s as temperature rises; and secondly, the maximum value of s being constrained to a value below one. The aforementioned results suggest that the transport mechanism of charges may be understood by using the correlated barrier hopping model, CBH. [19, 23]. The same mechanism was observed in many MPcs such as MgPc [13], Na_2Pc [14] ZnPc [15], CuPc [16], CoPc [17], and AlPcCl [19].

It is anticipated that the carrier will traverse the potential obstacle that exists between two adjacent places. According to this model, there is an inverse relationship between the temperature and the value of **s**, so that an increase in temperature leads to a drop in the value of **s** . The assigned value (referred to as "**s**") in the CBH model is constrained to the range of 0 to 1. In order to determine the potential barrier height (Wm) of the Coulomb potential barrier, one can employ the universal formula.

$$s = 1 - \frac{6k_B T}{W_M} \qquad (3)$$

This equation calculates $\mathbf{W_M}$ by graphing (**1-s**) versus **T**, as shown in **Fig. 6** and using the slope to calculate the binding energy, which was 0.11105 eV.

Fig. 7 depicts AC conductivity $\sigma_{ac}(\omega)$ as a function of reciprocal temperature at various frequencies. According to the figure, when temperature rises, $\sigma_{ac}(\omega)$ rises linearly. This demonstrates that the AC conductivity is a thermally activated operation that comes from distinct localized states in the gap [24]. The dependence of $\sigma_{ac}(\omega)$ on temperature is represented by.

$$\sigma_{ac}(\omega) = \sigma_o \exp\left(-\frac{\Delta E_{ac}}{KT}\right) \qquad (4)$$

where σ_o is a constant and ΔE_{ac} is conduction activation energy. The activation energy values found at various frequencies range from approximately 1.448 eV at about 600 Hz to 0.66 eV at 600 kHz.

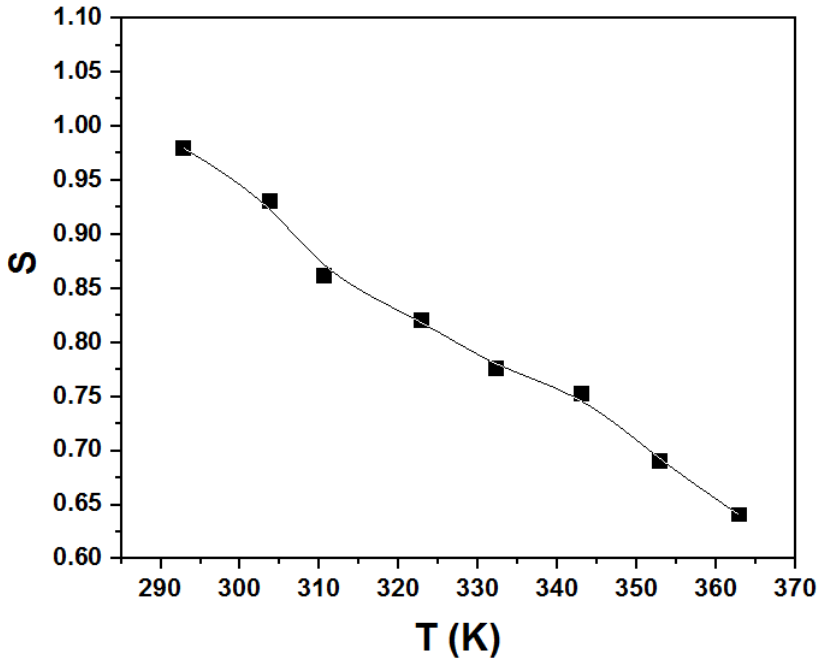

Fig.5. Temperature dependence of power exponent (s).

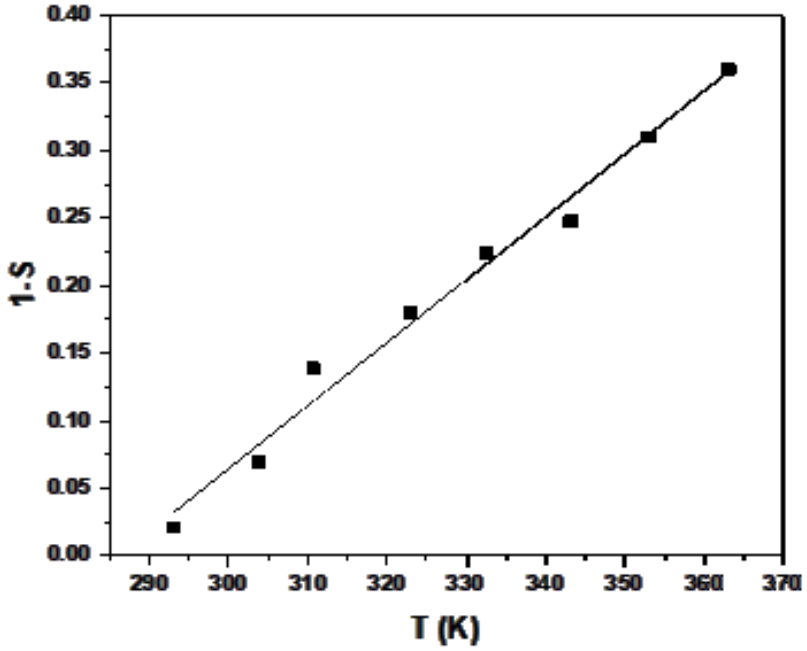

Fig.6. Temperature dependence of 1-s

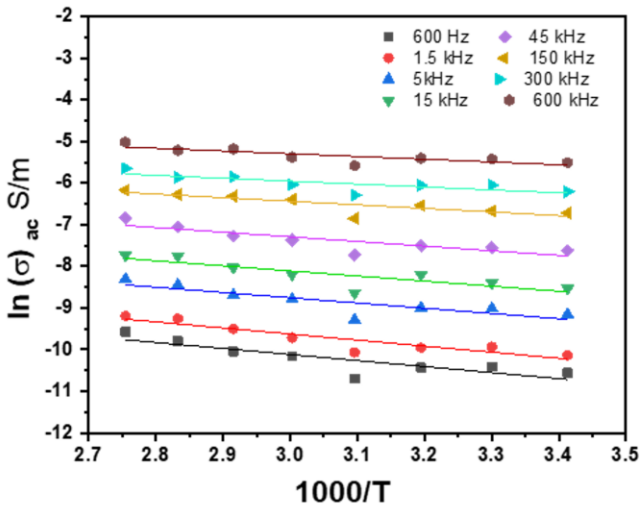

Fig. 7. Variation of AC conductivity, $\sigma_{ac}(\omega)$, with temperature at different frequencies for $TiPcCl_2$

Dielectric studies

The dielectric characteristics demonstrate a relationship with many types of polarisation, including electronic, ionic, relaxation, and space charge (25, 26). The study of dielectric properties of materials is of utmost importance in advancing our understanding of the electrical characteristics in relation to frequency and temperature. The expression for the complex permittivity ε* in this particular circumstance is provided in reference [27]:

$$\boldsymbol{\varepsilon^* = \varepsilon_1 - i\varepsilon_2} \qquad (5)$$

where $\boldsymbol{\varepsilon_1}$ is the dielectric constant and $\boldsymbol{\varepsilon_2}$ is the dielectric loss, the relation that combines each of them can be obtained by:

$$\boldsymbol{\varepsilon_2 = \varepsilon_1 \tan\delta} \qquad (6)$$

where **tanδ** (**δ=90-φ**) represents the dissipation factor.

The dielectric constant is computed using the following formula [27]:

$$\boldsymbol{\varepsilon_1 = \frac{d\,c}{A\,\varepsilon_0}} \qquad (7)$$

where C is the capacitance expressed in farad, d is the disc thickness and $\boldsymbol{\varepsilon_0}$ is the permittivity of free space. Lastly, A denotes the cross-sectional area of the disc. The dielectric measurements were performed at temperatures ranging from (293K to 363K), and at frequencies from (50 HZ to 5 MHz). **Fig. 8** illustrates the frequency dependence of $\boldsymbol{\varepsilon_1}$. The figure demonstrates a clear that as the frequency increases, $\boldsymbol{\varepsilon_1}$ decreases. At comparatively high temperatures

with low frequencies, the dielectric constant exhibits a significant dependency on frequency, whereas the variation is minimal at high frequencies and low temperatures, as explained that at lower frequencies. The determination of $\boldsymbol{\varepsilon_1}$ in polar materials may be attributed to the combined impact of many elements that contribute to polarizability. These factors include relaxation polarisation (both interfacial and orientational) as well as deformational polarisation (both ionic and electronic). The increase in frequency leads to a decrease in the ability of dipoles to rotate quickly, This further increase in frequency causes the dipoles to lose their ability to orient themselves and they become unable to respond to the applied field. Consequently, the decrease in $\boldsymbol{\varepsilon_1}$ at higher frequencies approaches a constant value, which is a result of interfacial polarization [25].

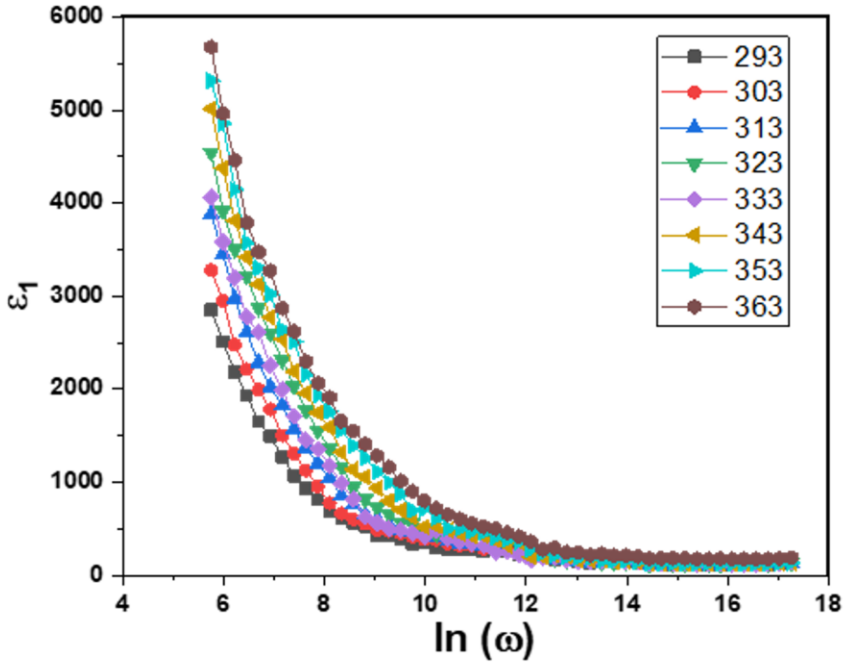

Fig. 8. Variation of the dielectric constant ε_1 with frequencies at different temperatures for $TiPcCl_2$

The frequency-dependent behavior of the dielectric loss $\boldsymbol{\varepsilon_2}$, is seen in **Fig. 9**. From the figure $\boldsymbol{\varepsilon_2}$ it can be observed that the values exhibit similar behavior as ε_1. The primary sources of dielectric losses are often recognized as dipole losses, dielectric losses, and conduction losses [19]. The rise in temperature is leads to a corresponding increase in electrical conduction losses, hence causing a rise in the magnitude of dielectric loss.

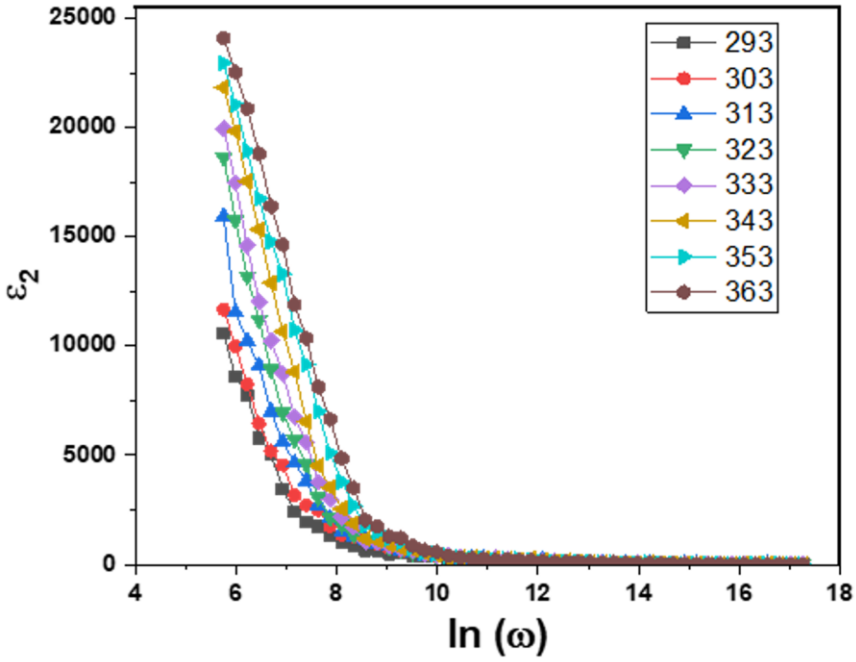

Fig. 9. Variation of the dielectric loss ε_2 with frequencies at different temperatures for $TiPcCl_2$

Electric modulus study

The electric modulus, represented by M*, may serve as an alternate approach to defining the dielectric qualities, offering a valuable viewpoint on these features. By comparing the electric modulus, M*, with the complex dielectric permittivity, ε*, it becomes possible to distinguish between long-range electrical conductivity and local dielectric relaxation phenomena, such as dipole reorientation (as shown by reference) [28]. By using the modulus representation, unwanted effects caused by extrinsic relaxations can be reduced to a minimum. The complex electric modulus is obtained by the derivation of the equation for complex permittivity [29]. According to Macedo et al [19], the real and imaginary parts of the electric modulus $\mathbf{M}^{`}$ and $\mathbf{M}^{``}$ can be determined from $\boldsymbol{\varepsilon_1}$ and $\boldsymbol{\varepsilon_2}$ as follows:

$$\boldsymbol{M^*} = \frac{\mathbf{1}}{\boldsymbol{\varepsilon^*}} = \boldsymbol{M`} + \boldsymbol{jM``} \quad (8)$$

where:

$$\boldsymbol{M`} = \frac{\boldsymbol{\varepsilon_1}}{[(\boldsymbol{\varepsilon_1})^2+(\boldsymbol{\varepsilon_2})^2]} \quad (9)$$

$$\boldsymbol{M``} = \frac{\boldsymbol{\varepsilon_2}}{[(\boldsymbol{\varepsilon_1})^2+(\boldsymbol{\varepsilon_2})^2]} \quad (10)$$

Figure 19 illustrates the relationship between $\mathbf{M}'$ and frequency at different temperatures. The values of $\mathbf{M}'$ in the low-frequency domain are typically zero, which provides confirmation of the occurrence of electrode polarisation

phenomena [30]. The dispersion of $\mathbf{M}'$ exhibits a positive correlation with frequency, and at elevated frequencies, it demonstrates a tendency to remain consistent across various temperature conditions. The observed phenomenon could potentially be attributed to the short-range mobility of charge carriers. **Fig. 11** displays the frequency function of **M"** at different temperatures. The observed variation in the third derivative of the magnetization, **M"** with respect to frequency suggests that an increase in temperature leads to a displacement of the relaxation peaks towards higher frequencies. The existence of relaxation processes with varying time constants, as shown by the asymmetric widening of the M' 'peaks', supports the occurrence of non-Debye relaxation in our experimental sample [31]. Also, the same relaxation processes was observed in bulk AlPcCl [19].

The frequency range preceding the peak maximum exhibits a change from long-range to short-range mobility as frequency increases. In order to quantify the typical relaxation time, it is possible to adopt the reciprocal of the frequency at the maximum position as a practical metric, denoted as $\boldsymbol{\tau_m = \omega_m^{-1}}$. Hence, the relationship between temperature and the characteristic relaxation time may be ascertained, as seen in **Fig.12**, which exhibits the Arrhenius relation [32]:

$$\boldsymbol{\omega_m = \omega_0 \, exp(-\Delta E_\omega \, / \, K_B T)} \qquad (11)$$

where ω_0 is the pre-exponent factor, ΔE_ω is the activation energy for dielectric relaxation, which is about 4.456 eV.

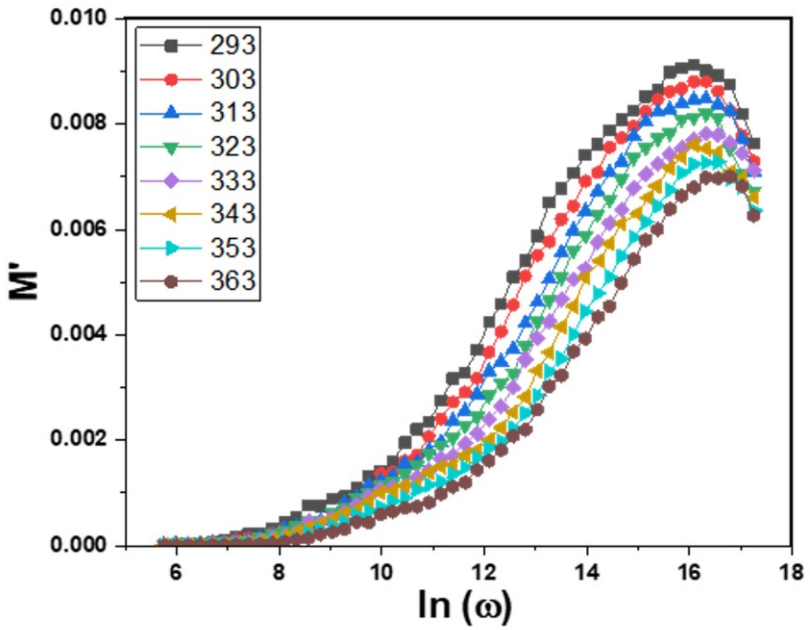

Fig. 10. Frequency dependence of M` of $TiPcCl_2$ different temperatures.

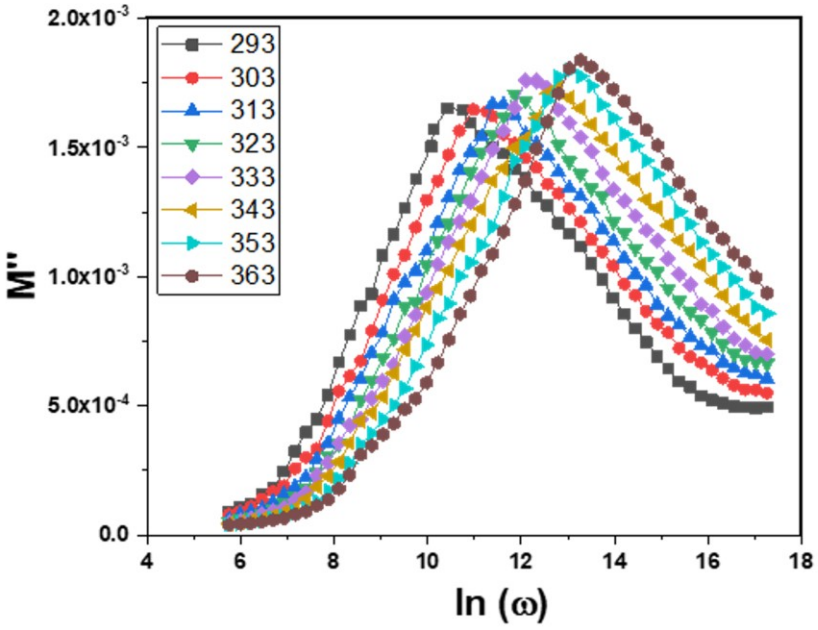

Fig. 11. Frequency dependence of M`` of $TiPcCl_2$ different temperatures.

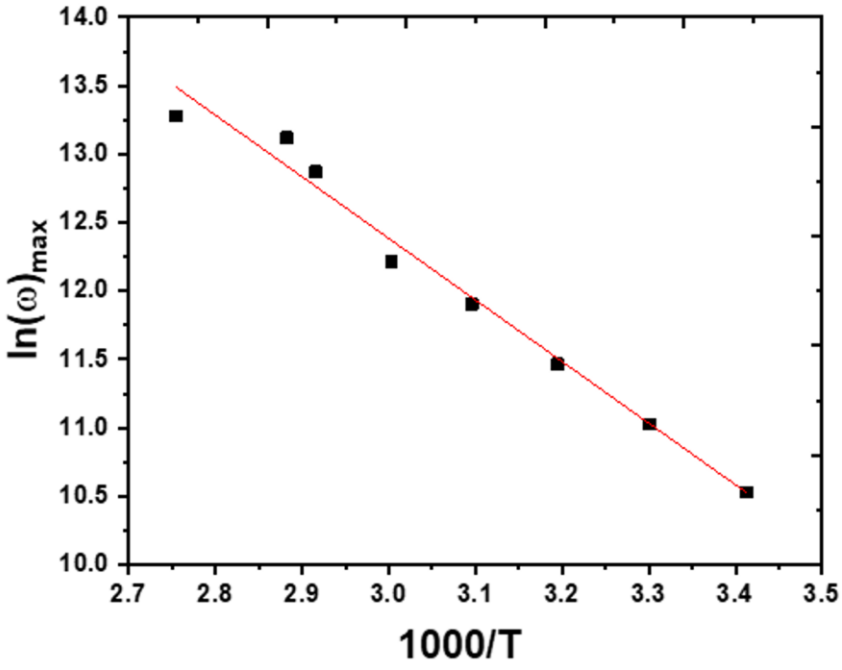

Fig. 12. Temperature dependence of the Debye peak position of Z ' for $TiPcCl_2$.

Conclusion

The current investigation focused on examining the impact of frequency and temperature on the electrical conductivity and dielectric relaxation of sandwich structures composed of Ag/$TiPcCl_2$/Ag. Throughout the frequency range of 50 Hz to 5 MHz, it was observed that the AC conductivity $\sigma_{ac}(\omega)$ varies with respect to $\boldsymbol{\omega^s}$. For high-frequency ranges, the frequency exponent exhibits a value $s < 1$. Furthermore, it is observed that when temperature increases, the frequency exponent decreases. These observations provide evidence that conduction is attributed to the correlated barrier hopping (CBH) process. The calculation yielded a maximum barrier height for hopping or the binding energy WM of 0.11105 eV. Both the real part $\varepsilon`$ and the imaginary part $\varepsilon``$ of the dielectric constant were shown to rise with temperature and fall with frequency. This behavior also demonstrated that the $TiPcCl_2$ sample consists of molecular dipoles. The utilisation of the electric modulus, denoted as M*, has been proposed as an alternate approach for quantifying the dielectric characteristics of a substance. The observed relationship between the frequency variation of M" and temperature revealed a notable trend: as the temperature increased, the relaxation peaks exhibited a shift towards higher frequencies. The activation energy for dielectric relaxation, ΔE_ω, was found to be about 4.456 eV. Based on the obtained data, it can be concluded that $TiPcCl_2$ has promising characteristics for use in storage applications.

References

[1] WoongNamgoong, J., MoKim, H., PilKim, S. H., BumYuk, JunChoi, and Jae, S. "Synthesis and characterization of metal phthalocyanine bearing carboxylic acid anchoring groups for nanoparticle dispersion and their application to color filters," *Dye. Pigment.*, vol. 184, p. 108737, 2021.

[2] Halaskova, M. *et al.*, "Peripherally Crowded Cationic Phthalocyanines as Efficient Photosensitizers for Photodynamic Therapy," *Am. Chem. Soc.*, vol. 12, pp. 502–507, 2021.

[3] Chen, Q. *et al.*, "Tetraalkyl-substituted zinc phthalocyanines used as anode buffer layers for organic light-emitting diodes," *Chin. Phys. B*, vol. 29, p. 017302, 2020.

[4] Şahin, Z., Meunier-Prest, R., Dumoulin, F., Kumar, A., Isci, Ü. and Bouvet, M. "Tuning of organic heterojunction conductivity by the substituents' electronic effects in phthalocyanines for ambipolar gas sensors," *Sensors Actuators B Chem.*, vol. 332, p. 129505, 2021.

[5] Vasseur, K., Rand, B. P., Cheyns, D., Temst, K., Froyen, L. and Heremans, P. "Correlating the Polymorphism of Titanyl Phthalocyanine Thin Films with Solar Cell Performance," *J. Phys. Chem. Lett.*, vol. 3, pp. 2395–2400, 2012.

[6] Kumar, A. Vashistha, V. K. and Das, D. K. "Recent development on metal phthalocyanines based materials for energy conversion and storage applications," *Coord. Chem. Rev.*, vol. 431, p. 213678, 2021.

[7] Mansour, Sh.A., Yahia, I.S. and Yakuphanoglu, F. "The electrical conductivity and dielectric properties of C.I. Basic Violet 10," *Dye. Pigment.*, vol. 87, no. 2, pp. 144–148, 2010.

[8] Morsi, M.A., Rajeh, A. and Al-Muntaser, A.A. "Reinforcement of the optical, thermal and electrical properties of PEO based on MWCNTs/Au hybrid fillers: Nanodielectric materials for organoelectronic devices," *Compos. Part B Eng.*, vol. 173, p. 106957, 2019.

[9] Ghosh, A. "ac conduction in iron bismuthate glassy semiconductors," *Phys. Rev. B*, vol. 42, no. 2, p. 1388, 1990.

[10] Elliott, S. R. "A.c. conduction in amorphous chalcogenide and pnictide semiconductors," *Adv. Phys.*, vol. 36, no. 2, pp. 135–217, 1987.

[11] Enneffati, M., Louati, B., Guidara, K., Rasheed, M. and Barillé, R. "Crystal structure characterization and AC electrical conduction behavior of sodium cadmium orthophosphate," *J Mater Sci Mater Electron*, vol. 29, pp. 171–179, 2018.

[12] A.Timoumi *et al.*, "Electrical impedance spectroscopy study of unsubstituted palladium (II) phthalocyanine," *Synth. Met.*, vol. 272, p. 116659, 2021.

[13] Atta, A. A. "AC conductivity and dielectric measurements of bulk magnesium phthalocyanine (MgPc)," *J. Alloys Compd.*, vol. 480, no. 2, pp. 564–567, 2009, doi: 10.1016/j.jallcom.2009.01.124.

[14] Alosabi, A. Q. Al-Muntaser, A. A., El-Nahass, M. M. and Oraby, A. H. "Electrical conduction mechanism and dielectric relaxation of bulk disodium phthalocyanine," *Phys. Scr.*, vol. 97, no. 5, 2022, doi: 10.1088/1402-4896/ac5ff8.

[15] Zeyada, H. M. and El-Nahass, M. M. "Electrical properties and dielectric relaxation of thermally evaporated zinc phthalocyanine thin films," *Appl. Surf. Sci.*, vol. 254, no. 6, pp. 1852–1858, 2008, doi: 10.1016/j.apsusc.2007.07.175.

[16] Bahabri, F. S. and Ghamdi, A. A. A. L. "Structural and Transport Properties of Copper Phthalocyanine (CuPc) Thin Films," *Egypt. J. Solids*, vol. 25, no. 2, pp. 307–321, 2002, doi: 10.21608/ejs.2002.150486.

[17] Soliman, H. S. El-Barry, A. M. A., Khosifan, N. M. and El Nahass, M. M. "Structural and electrical properties of thermally evaporated cobalt phthalocyanine (CoPc) thin films," *Eur. Phys. J. - Appl. Phys.*, vol. 37, no. 1, pp. 1–9, 2007.

[18] Soliman, H. S., El Nahass, M. M., Farid, A. M., Farag, A. A. M. and El Shazly, A. A. "Structural and transport properties of evaporated iron phthalocyanine (FePc) thin films," *Eur. Phys. J. AP*, vol. 21, pp. 187–193, 2003.

[19] Soliman, I. M., El-Nahass, M. M. and Mansour, Y. "Electrical, dielectric and electrochemical measurements of bulk aluminum phthalocyanine chloride (AlPcCl)," *Solid State Commun.*, vol. 225, pp. 17–21, 2016, doi: 10.1016/j.ssc.2015.10.011.

[20] Papathanassiou, A. N., Sakellis, I. and Grammatikakis, J. "Universal frequency-dependent ac conductivity of conducting polymer networks," *Appl. Phys. Lett.*, vol. 91, p. 122911, 2007.

[21] Meikhail, M.S., Oraby, A.H., El-Nahass, M.M., Zeyada, H.M. and Al-Muntaser, A.A. "Electrical conduction mechanism and dielectric characterization of MnTPPCl thin films," *Phys. B Condens. Matter*, vol. 539, pp. 1–7, 2018.

[22] Makhlouf , M.M.and Zeyada, H.M. "Synthesis, structural analysis, spectrophotometric measurements and semiconducting properties of 3-phenyl azo-4-hydroxycoumarin thin films," *Synth. Met.*, vol. 211, pp. 1–13, 2016.

[23] Mostafa Saad Ebied, Mohammed Nassary, "AC conductivity and dielectric measurements of bulk Coumarin-

6," *IOSR J. Appl. Phys.*, vol. 14, no. 3, pp. 25–34, 2022, doi: 10.9790/4861-1403022534.

[24] Farid, A.M. and Bekheet, A.E. "AC conductivity and dielectric properties of Sb2S3 films," *Vacuum*, vol. 59, no. 4, pp. 932–939, 2000.

[25] Kao, K. C. *Dielectric Phenomena in Solids*. 2004.

[26] Harper, C. A. "Handbook of ceramics, glasses and diamonds," *McGraw-Hill*, 2001.

[27] El-Nahass, M. M. and Ali, H. A. M. "AC conductivity and dielectric behavior of bulk Furfurylidenemalononitrile," *Solid State Commun.*, vol. 152, no. 12, pp. 1084–1088, 2012.

[28] Dutta, A., Sinha, T. and Chandrahas, B. "Dielectric relaxation and ac conductivity study in SrMg1/3Nb2/3O3," *Indian J. Eng. Mater. Sci.*, vol. 15, pp. 181–186, 2008.

[29] Soares, B. G., Leyva, M. E., Barra, G. M. O. and Khastgir, D. "Dielectric behavior of polyaniline synthesized by different techniques," *Eur. Polym. J.*, vol. 42, no. 3, pp. 676–686, 2006.

[30] El-Denglawey, A., Qashou, S. I., Darwish, A. A. A. and El-Zaidia, E. F. M. "Phase, AC conductivity and dielectric properties of Indeno[1,2-b] flourene-6,12 dione thin film as a function of frequency and temperature," *Phys. Scr.*, vol. 96, no. 7, 2021, doi: 10.1088/1402-4896/abfcf2.

[31] Howell, F. S., Bose, R. A., Macedo, P. B. and Moynihan, C. T. "Electrical relaxation in a glass-forming molten salt," *J. Phys. Chem.*, vol. 78, no. 6, pp. 639–648, 1974.

[32] Buraidah M. H., Teo, L. P., Majid, S. R.and Arof, A. K. "Ionic conductivity by correlated barrier hopping in NH4I doped chitosan solid electrolyte," *Phys. B Condens. Matter*, vol. 404, no. 8–11, pp. 1373–1379, 2009.